Hearing Research 283 (2012) 45–58

Contents lists available at SciVerse ScienceDirect

Hearing Research

journal homepage: www.elsevier.com/locate/heares

Research paper

# Cochlear-implant spatial selectivity with monopolar, bipolar and tripolar stimulation

Ziyan Zhu [a,b,c,*], Qing Tang [c], Fan-Gang Zeng [c,**], Tian Guan [b], Datian Ye [a,b,*]

[a] Department of Biomedical Engineering, School of Medicine, Tsinghua University, Beijing 100084, China
[b] Research Center of Biomedical Engineering, Graduate School at Shenzhen, Tsinghua University, Shenzhen, Guangdong 518055, China
[c] Department of Biomedical Engineering, University of California, Irvine, CA 92697, USA

ARTICLE INFO

*Article history:*
Received 13 August 2010
Received in revised form
28 October 2011
Accepted 8 November 2011
Available online 22 November 2011

ABSTRACT

Sharp spatial selectivity is critical to auditory performance, particularly in pitch-related tasks. Most contemporary cochlear implants have employed monopolar stimulation that produces broad electric fields, which presumably contribute to poor pitch and pitch-related performance by implant users. Bipolar or tripolar stimulation can generate focused electric fields but requires higher current to reach threshold and, more interestingly, has not produced any apparent improvement in cochlear-implant performance. The present study addressed this dilemma by measuring psychophysical and physiological spatial selectivity with both broad and focused stimulations in the same cohort of subjects. Different current levels were adjusted by systematically measuring loudness growth for each stimulus, each stimulation mode, and in each subject. Both psychophysical and physiological measures showed that, although focused stimulation produced significantly sharper spatial tuning than monopolar stimulation, it could shift the tuning position or even split the tuning tips. The altered tuning with focused stimulation is interpreted as a result of poor electrode-to-neuron interface in the cochlea, and is suggested to be mainly responsible for the lack of consistent improvement in implant performance. A linear model could satisfactorily quantify the psychophysical and physiological data and derive the tuning width. Significant correlation was found between the individual physiological and psychophysical tuning widths, and the correlation was improved by log-linearly transforming the physiological data to predict the psychophysical data. Because the physiological measure took only one-tenth of the time of the psychophysical measure, the present model is of high clinical significance in terms of predicting and improving cochlear-implant performance.



## 1. Introduction

Spatial selectivity, or frequency tuning in acoustic hearing, has played a pivotal role in auditory research and practice for over 100 years (Helmholtz, 1877). The concept of spatial selectivity has been used to explain a wide range of auditory phenomena from loudness, pitch and masking to music and speech perception (e.g., Fletcher, 1935; Plomp, 1964). Spatial selectivity can be characterized either directly by physiological means (e.g., Bekesy, 1952; Tasaki, 1954) or indirectly by psychophysical means (e.g., Chistovich, 1957; Small, 1959; Zwicker, 1974). There is generally good correspondence between physiologically and psychophysically measured spatial selectivity, as sharp tuning is observed with normal hearing whereas broad tuning is observed with sensorineural hearing loss (e.g., Liberman and Dodds, 1984; Moore and Glasberg, 1986).

Spatial selectivity has also played an important role in the development of modern multichannel cochlear implants (CI), which can restore significant functional hearing to deaf people by conveying acoustic spectral information to different places in the cochlea. However, compared with 3000 tonotopically-organized inner hair cells and their sharp tuning (e.g., Ruggero, 1992), the amount of spectral information in a cochlear implant is severely limited by not only the small number of intracochlear electrodes but also the wide spread of electrical stimulation and nerve survival (e.g., Finley et al., 2008; Khan et al., 2005; Shannon, 1983; Wilson et al., 1991; Zeng, 2004). As a result, the actual number of independent channels is significantly smaller than the number of physical electrodes in a cochlear implant (e.g., Fishman et al., 1997;

* Corresponding authors. Department of Biomedical Engineering, School of Medicine, Tsinghua University, Beijing 100084, China.
** Corresponding author. Tel.: +1 949 824 1539.
*E-mail addresses:* zhuzy05@mails.tsinghua.edu.cn (Z. Zhu), fzeng@uci.edu (F.-G. Zeng), yedt6386@sz.tsinghua.edu.cn (D. Ye).

0378-5955/$ – see front matter © 2011 Elsevier B.V. All rights reserved.
doi:10.1016/j.heares.2011.11.005

**Table 1**
Subject demographical information and speech performance. HINT stands for hearing in noise test. The first column in HINT represents test scores in quiet and the second column represents scores at 5-dB signal-to-noise ratio.

| Subject | Gender | Age (yrs) | Etiology | Deafness duration (yrs) | CI use (yrs) | Device type | HINT (% correct) | |
|---|---|---|---|---|---|---|---|---|
| S1 | M | 67 | Meningitis | 59 | 7 | CII | 72 | 33 |
| S2 | F | 72 | Familial | 55 | 8 | CII | 91 | 40 |
| S3 | M | 50 | Unknown | 1 | 4 | 90K | 80 | 0 |
| S4 | F | 53 | Unknown | 41 | 4 | 90K | 50 | 5 |
| S5 | F | 55 | Congenital | 48 | 7 | CII | 0 | 0 |
| S6 | F | 72 | Progressive | 9 | 2 | 90K | 100 | 70 |

Friesen et al., 2001); the CI users' ability to resolve spectral contrast is also highly variable and can be directly correlated to their speech performance in quiet and in noise (Henry and Turner, 2003; Litvak et al., 2007b; Won et al., 2007).

The need to increase the number of functional channels in cochlear implants has spurred extensive research from new electrode designs to advanced signal processing (e.g., Koch et al., 2004; Tykocinski et al., 2001). Recent attention has been paid to manipulating electrode configuration and stimulation delivery to steer or focus the electrical field (for a review, see Bonham and Litvak, 2008). In particular, different electrode configurations have shown successively more focused electrical fields from monopolar, bipolar, to tripolar stimulation (e.g., Jolly et al., 1996; Kral et al., 1998; Zhu et al., 2010). The increased spatial selectivity with bipolar and tripolar stimulation modes is also supported by physiological studies in the auditory nerve (Kral et al., 1998; Miller et al., 2003; van den Honert and Stypulkowski, 1987), the inferior Colliculus (Bierer et al., 2010; Bonham and Litvak, 2008; Snyder et al., 2008), and the auditory cortex (Bierer and Middlebrooks, 2002; Middlebrooks and Bierer, 2002; Raggio and Schreiner, 1994). Therefore, it seems reasonable to hypothesize that focused stimulation such as bipolar and tripolar configurations will increase functional spatial selectivity and hopefully improve the overall cochlear-implant performance.

Unfortunately, this hypothesis has not been established functionally as recent studies showed little or no improvement in cochlear-implant performance using focused electric stimulation (Berenstein et al., 2008; Donaldson et al., 2011; e.g., Mens and Berenstein, 2005; Pfingst et al., 2001). There are several explanations for this lack of correspondence between physical and functional measures of focused stimulation. First, focused stimulation requires a higher current level than monopolar stimulation to reach behavioral threshold and comfortable loudness, so the benefit of focused stimulation may be reduced with the increased level of input (e.g., Berenstein et al., 2010; Chua et al., 2011; Kwon and van den Honert, 2006; Pfingst and Xu, 2004). Second, there are significant differences in physiological and psychophysical methods in addition to differences in animal and human studies of spatial selectivity. For example, psychophysical methods usually employed longer stimulation duration than physiological methods, which typically used single pulses (e.g., Abbas et al., 2004; Hughes and Stille, 2008; Lim et al., 1989). Animal studies typically used acute preparations with relatively good nerve survival while human studies usually involved patients with longer duration of deafness, which is a likely indication of poor nerve survival, both of which could significantly influence spatial selectivity (e.g., Goldwyn et al., 2010; Linthicum et al., 1991; Nadol et al., 2001; Vollmer et al., 2007). Third, there is a great deal of individual variability from etiology to performance that often renders direct comparison of psychophysical and physiological spatial selectivity difficult, if not impossible. For example, the first study of psychophysical spatial tuning curve used Nucleus users in bipolar mode and Clarion users in monopolar mode, with different electrode arrays, electrode-to-electrode spacing, and reference electrodes (Nelson et al., 2008). Most notably, reliable psychophysical measures are usually not obtainable in the growing population of pediatric cochlear-implant users, requiring physiological measures that can accurately and reliably predict corresponding pediatric psychophysical and functional performance. An ideal study would obtain comparable physiological, psychophysical and speech measures using the same electric stimulation parameters in the same cohort of subjects so that the hypothetic link between cochlear-implant performance and physiological or psychophysical spatial selectivity can be directly addressed.

As a first goal, the present study directly compared psychophysical and physiological spatial selectivity under a controlled paradigm. To reduce variability between subjects, all measures were conducted in the same subjects using the same device. To control procedural differences, both psychophysical and physiological measures used a similar forward-masking paradigm, except for the use of pulse trains for psychophysical measurement and the use of single pulses for the physiological measurement. To control stimulus differences, all pulses had the same, but relatively long, pulse duration to achieve sufficient loudness in focused stimulation. In addition, loudness growth was measured for both pulse trains and single pulses to assure presentation of probe and masker at a proper level within their respective dynamic ranges. The second goal was to test whether, under these stringent conditions, there were significant differences in spatial selectivity between broad and focused electric stimulation modes. The final goal was to test whether the psychophysical spatial tuning could be predicted from the physiological spatial masking curve.

## 2. Methods

### 2.1. Subjects

Six cochlear-implant users, using either a Clarion II or a HiRes90K device (Advanced Bionics Corp., Valencia, CA), participated in this study. All subjects had a HiFocus J electrode array consisting of 16 intracochlear electrodes numbered from the most apical (EL1) to the most basal (EL16) position, with a center-to-center electrode distance of 1.1 mm. All subjects were native speakers of American English and were postlingually deafened except S5. S3 received the implant to control tinnitus and had normal hearing on the non-implant side (Cullington and Zeng, 2010; Zeng et al., 2011). S4 had 4 disabled electrodes (EL13-16) due to high impedance. S6 was a bilateral cochlear-implant user with a Clarion I device on one side and a HiRes90K device on the other. Only the HiRes90K device was used because the Clarion I lacked telemetry capabilities. Table 1 displays subject demographic information and speech performance. The present study was conducted in accordance with guidelines set by the Institutional Review Board of University of California, Irvine.

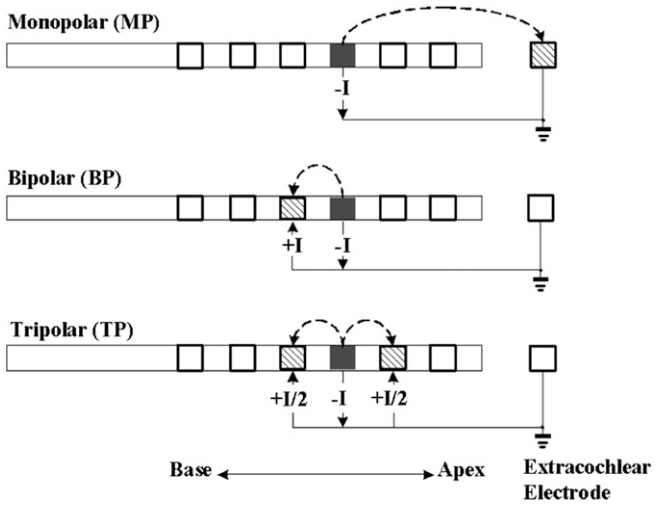


**Fig. 1.** A schematic diagram of three stimulation modes. Monopolar (top), bipolar (middle), and tripolar (bottom) stimulations all have the same active electrode (gray bar; EL = electrode), but different return electrodes (hatched bars; EL − 1 or EL + 1 or EC = extra-cochlear electrode). The solid lines indicates the electric circuit; the dashed arrow represents the current path from active to return electrode, with (−I) indicating the cathodic phase.

### 2.2. Stimulation modes

Fig. 1 shows monopolar, bipolar, and tripolar stimulation modes, which had the same intracochlear active electrode (EL8) but different returning or reference electrodes. The monopolar mode used an extracochlear electrode placed in the temporalis muscle as the reference. The bipolar mode used an adjacent intracochlear electrode (EL9), basal to the active electrode, as the reference. The tripolar mode used two adjacent electrodes (EL7 and EL9) as references, with each receiving half of the current delivered to the active electrode. The Bionic Ear Data Collection System (BEDCS, V1.17.208, Advanced Bionics Corp.) was used to present the stimuli, and record subject response and telemetry information.

The forward-masked spatial tuning curve has emerged as a psychophysical method of choice in both acoustic and electric hearing for its ability to not only characterize the sharpness of spatial selectivity but also identify the underlying nerve survival pattern, such as dead regions (e.g., Dingemanse et al., 2006; Moore and Alcantara, 2001; Nelson et al., 2008). On the other hand, a forward-masking subtraction method to measure electrical compound action potentials (ECAP, see Abbas et al., 2004; Miller et al., 2000) has been used to characterize the physiological spatial masking curve, a counterpart of the psychophysical spatial tuning curves (Cohen et al., 2003; Saoji et al., 2009). Both the spatial tuning and masking curve measures fix the probe position while varying the masker position. However, they differ in terms of the criterion used to characterize the spatial selectivity. The spatial tuning curve method varies the masker level to render a fixed-level probe just inaudible, producing an “iso-response” curve, whereas the spatial masking curve method fixes the masker level to measure its effect on a fixed-level probe response, producing an “iso-input” curve (Pickles, 1988). If the system is linear, then the iso-response curve can be derived by simply inverting the iso-input curve, or vice versa.

### 2.3. Psychophysical spatial tuning curve

The forward-masking paradigm has been previously used in the past and will be briefly described here (e.g., Chatterjee and Shannon, 1998; Nelson and Donaldson, 2002; Nelson et al., 2008; Shannon, 1983). The masker duration was 160 ms, and the probe duration was 10 ms. The masker-probe delay, between masker offset and probe onset, was 10 ms. The masker and the probe were both 500 Hz pulse trains. At a single-pulse level, the biphasic pulses were always charge-balanced with cathodic-leading phase and zero inter-phase delay. Based on previous studies, long phase duration of 226.4 μs was chosen to achieve comfortable loudness within the compliance limit in the implant device, which could be a problem, especially with tripolar stimulation (e.g., Bierer et al., 2010; Chua et al., 2011; Litvak et al., 2007a; Srinivasan et al., 2010).

Loudness growth from thresholds (THS) to maximum acceptable loudness (MAL) was measured for both the 160-ms masker and the 10-ms probe prior to spatial tuning curve data collection. The threshold was obtained using a three-interval forced choice (3IFC) adaptive procedure with a two-down, one-up decision rule to estimate the stimulus level corresponding to 70.7% correct detection (Levitt, 1971). The MAL was obtained using an ascending method of limits procedure, in which the pulse train, presented at a rate of 1/s, was increased in amplitude until the subject indicated his or her maximal comfortable loudness (Shannon, 1985). Loudness was estimated for 5–9 stimulus levels spanning over the entire dynamic range. Each procedure was repeated 3–5 times to obtain an average value. Fig. 2 shows individual loudness growth as a function of current level for the 160-ms (filled squares) and 10-ms (open inverted triangles) stimuli. Except for S3 with bipolar and tripolar stimulation, which displayed an exponential loudness growth, the remaining data can be nicely fitted with a logarithmic function (e.g., Chua et al., 2011; Fu, 2005; Zeng and Shannon, 1992, 1994). Excluding the tail in S3 yielded a mean slope of 7.2 (SE = 0.6) for the 160-ms probe and 8.5 (SE = 0.7) for the 10-ms probe, with no significant difference between the two duration conditions ($t_{17} = 1.59$, $p = 0.13$). Including the tail would produce a poorer fit to the data (e.g., see the solid line in S3 tripolar case) and would slightly decrease the mean values but still produce no significant difference between the two duration conditions.

Table 2 shows the averaged threshold, MAL and dynamic range values from all 6 subjects under the 2 stimulus durations and 3 stimulation modes. Within-subjects repeated-measures ANOVA indicated a significant effect of stimulation mode on the 160-ms masker thresholds ($F_{2,70} = 886.3$, $p < 0.01$) and MAL ($F_{2,70} = 554.6$, $p < 0.01$). The averaged masker threshold, or MAL, was the lowest in monopolar stimulation, followed by an increase by about 12 dB in bipolar stimulation, and followed by an additional 5 dB in tripolar stimulation. A similar difference in stimulation mode was also observed for the averaged 10-ms probe threshold ($F_{2,10} = 10.1$, $p < 0.01$) and MAL ($F_{2,10} = 11.5$, $p < 0.01$). However, the averaged dynamic range was not significantly different as a function of stimulation mode for either the masker (8–9 dB: $F_{2,70} = 5.8$, $p = 0.06$) or the probe (8–10 dB: $F_{2,10} = 0.54$, $p = 0.59$).

The spatial tuning curve was measured at each of the following three probe levels: 5–10%, 15–20%, or 25–33% of the dynamic range. The forward masker level required to mask the probe was estimated using a 3IFC adaptive procedure, in which the forward masker was presented in all three intervals and the probe was presented in one of the three intervals, chosen at random. The subject’s task was to choose the interval that contained the probe. Trial-by-trial feedback regarding the correct response was provided. The amplitude of the masker was initially set to a level 2–4 dB below the anticipated forward-masked threshold. A two-up, one-down decision rule was used, with an initial step of 1 dB for the first 4 reversals and 0.25 dB for the remaining reversals. A run contained 50 trials or fewer if 12 reversals were achieved. The mean of the final even number of reversals within the 50 trials, or 8 reversals when less than 50 trials were used, was taken as the

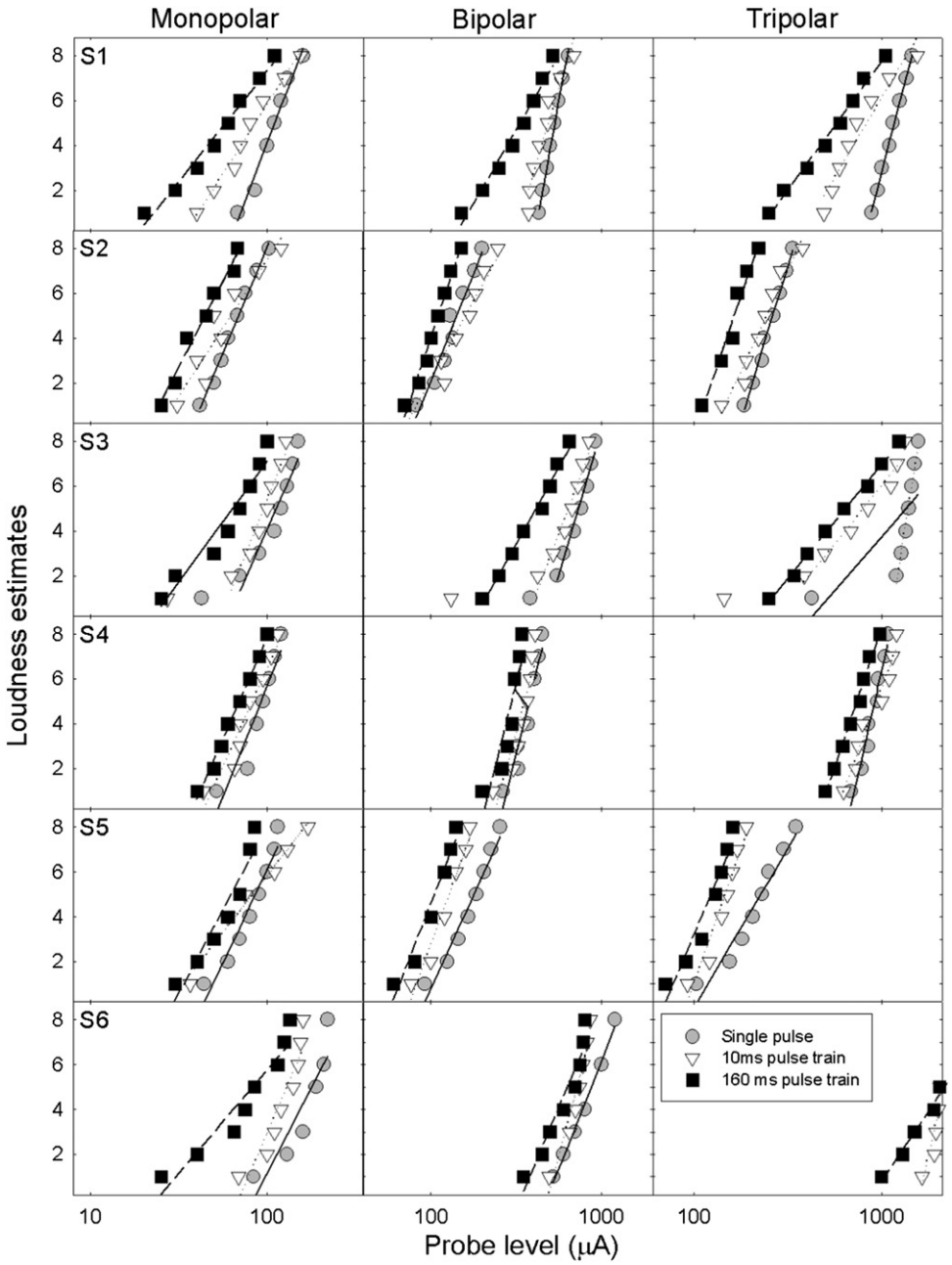


**Fig. 2.** Individual loudness growth (rows) as a function of logarithmic current level (*x*-axis) using three stimulation modes (columns) and three stimulation durations (symbols). The data were fitted using a logarithmic function (see text for details).

**Table 2**
Threshold, maximal loudness level (MAL), and dynamic range for pulse trains used in the psychophysical spatial tuning curve paradigm. All values were shown as mean ± SE and in dB re: 1 μA.

| | Threshold | MAL | Dynamic range |
|---|---|---|---|
| 160-ms Masker | | | |
| Monopolar | 30.7 ± 0.27 | 39.8 ± 0.19 | 9.3 ± 0.22 |
| Bipolar | 43.7 ± 0.54 | 52.0 ± 0.48 | 8.3 ± 0.26 |
| Tripolar | 48.8 ± 0.75 | 57.8 ± 0.66 | 9.0 ± 0.10 |
| 10-ms Probe | | | |
| Monopolar | 32.1 ± 1.2 | 42.5 ± 0.54 | 10.3 ± 1.0 |
| Bipolar | 44.9 ± 2.9 | 53.0 ± 2.5 | 8.1 ± 1.8 |
| Tripolar | 49.9 ± 4.0 | 58.3 ± 3.2 | 8.3 ± 2.4 |

forward masker level that just masked the probe. The reported value of the forward masker level was averaged over 3–5 such runs.

### 2.4. Physiological spatial masking curve

Different from pulse trains used in the psychophysical spatial tuning curve paradigm, the physiological spatial masking curve paradigm used a single pulse for both masker and probe, thus requiring independent measurements of thresholds and MALs. Fig. 2 shows individual loudness growth as a function of current level of the single pulse (circles). Compared with both long-duration pulse-train stimuli, the single-pulse stimulus produced significantly steeper loudness growth with a mean slope of 10.9 ($SE = 1.1$; $t_{16} = 2.3$, $p < 0.05$). This slope difference in loudness

**Table 3**
Threshold, maximal loudness level (MAL), and dynamic range for a single pulse used in the physiological ECAP paradigm. All values were shown as mean ± SE and in dB re: 1 μA.

| Single-pulse masker or probe | Threshold | MAL | Dynamic range |
|---|---|---|---|
| Monopolar | 36.9 ± 0.20 | 43.4 ± 0.11 | 6.5 ± 0.21 |
| Bipolar | 50.5 ± 0.58 | 55.9 ± 0.44 | 5.4 ± 0.21 |
| Tripolar | 55.5 ± 0.91 | 60.1 ± 0.50 | 4.6 ± 0.44 |

growth between pulse-train and single-pulse stimuli didn't change with the tail adjustment for S3 and will be used to help account for variability of prediction of the spatial tuning curve from spatial masking curve (see Discussion later).

Table 3 details the averaged threshold, MAL and dynamic range values as a function of stimulation mode. Within-subjects repeated-measures ANOVA showed a significant effect of stimulation mode on all three behavioral measures ($F_{2,10} > 35.1$, $p < 0.01$). The average threshold was the lowest with monopolar stimulation, increased by about 13 dB with bipolar stimulation, and by an additional 5 dB with tripolar stimulation. Compared with the threshold change as a function of stimulation mode, the average MAL was increased at a shallower rate, resulting in a systematic decrease in the average dynamic range from monopolar stimulation to tripolar stimulation. Overall, this difference in loudness growth between a pulse train and a single pulse reflects different temporal integration between threshold and MAL measures (Donaldson et al., 1997; Zeng et al., 1998).

A forward-masking subtraction paradigm was utilized to eliminate artifact and to record ECAP signals (Abbas et al., 2004; Abbas et al., 1999; Brown et al., 2000; Cohen et al., 2003; de Sauvage et al., 1983; Dillier et al., 2002). In this paradigm, both masker and probe were a single biphasic pulse, with the masker preceding the probe by 452.8 μs. The BEDCS used a 9-bit analog-to-digital converter that had a pre-amplifier with 1000-dB gain and a 55-kHz sample rate. ECAP was recorded from two electrodes (EL6 and E10) that were located on each side of the active electrode (EL8). The case (IE1 in Clarion II device and IE2 in HiRes90K device) was used as the reference. The final reported ECAP value was the average from the two recording electrodes, with each having 64 sweeps. To obtain the physiological spatial masking curve at a fixed probe (i.e., EL8), the ECAP amplitude was measured as a function of the masker electrode from apex to base. The probe level was also fixed at 30%, 40%, 50%, or 60% of the dynamic range, while the masker level was always presented at the MAL or 100% of the dynamic range. Selection of these moderate probe levels and high masker level reflected a compromise between noise floor and masking effects. The reported spatial masking curve is the ECAP amplitude of the probe alone minus the forward-masked ECAP amplitude. If there is a significant overlap in excited neural population between the forward masker and the probe, e.g., they were close to one another, the spatial masking curve will reflect mostly the activity of the probe alone; if there was a minimal overlap between the two, the amplitude of the probe alone will be similar to the amplitude of the forward-masked ECAP, resulting a near zero spatial masking curve measure.

### 2.5. Data analysis

Following the definition and methods used by Nelson et al. (2008), a linear model was used to fit the slope from both apical and basal sides of the spatial tuning curve or masking curve. To determine the range of apical or basal electrodes used for the linear fit, the following two criteria had to be met: (1) The fit was statistically significant ($p < 0.05$), and (2) The range either produced the maximal $R^2$ if $R^2 \leq 0.90$ or included the largest number of electrodes if several ranges produced $R^2 > 0.90$. $Q_{1dB}$, defined as the bandwidth in terms of electrode distance that was either 1 dB above the tuning tip or 1 dB below the masking peak, was used as the measure of spatial selectivity.

One critical issue examined here was how to predict the psychophysical spatial tuning curve from the physiological spatial masking curve. Because psychophysical tuning curve is based on both peripheral input and central processing, it is logical to assume not only a correlation, but also more strongly a predictive transformation, between psychophysical tuning and physiological masking curves. Five different transformations including linear, logarithmic, exponential, power, and linear-logarithmic functions, were examined, with the linear-logarithmic transformation producing the closest prediction (see Section 3.3.):

$$\mathrm{STC} = 100 - A\frac{\mathrm{SMC}^{\theta} - 1}{\theta} + B, \quad (1)$$

where STC represents the predicted psychophysical spatial tuning curve data and SMC represents the measured physiological spatial masking data; $A$ (scaling factor), $B$ (DC factor), and $\theta$ ($0 < \theta \leq 1$, nonlinear factor) are the three free parameters to be estimated by minimizing the root-mean-square error between the measured and predicted psychophysical spatial tuning curve data. Eq. (1) is called the linear-logarithmic function because it becomes a linear function when $\theta = 1$:

$$\mathrm{STC} = 100 - A(\mathrm{SMC} - 1) + B, \quad (2)$$

Eq. (1) becomes a logarithmic function when $\theta$ approaches 0:

$$\mathrm{STC} = 100 - A\ln(\mathrm{SMC}) + B, \quad (3)$$

## 3. Results

### 3.1. Psychophysical spatial tuning curves

Fig. 3 shows 54 raw spatial tuning curves plotting masker level (dB re: 1 μA) as a function of masker electrode position, with rows representing individual subjects and columns representing stimulation modes. The three different symbols represent three different probe levels. The dotted vertical line represents the probe position at EL8. Despite the variability in individuals and stimulation modes, most spatial tuning curves exhibited a V shape with a tip close to the probe position. A linear model was used to fit spatial tuning curves at each of the 3 probe levels ($R^2 = 0.99 \pm 0.03$, range = 0.78–1.00, $p < 0.05$). The probe level produced a significant effect on the mask level at the tuning tip ($F_{2,51} = 5.8$, $p < 0.01$), but no significant effects on the bandwidth, slope, or tip position ($F_{2,51} \leq 0.4$, $p > 0.7$). This lack of the effect of probe level suggests two things. First, different from the nonlinear psychophysical spatial tuning curves in acoustic hearing, spatial tuning curves in electric hearing are linear or independent of the probe level. Second, the 3 spatial tuning curves, once adjusted by the probe level, can be averaged to reduce variability for further analysis of the other spatial tuning curve parameters.

Fig. 4 shows such averaged spatial tuning curves over the three probe levels (circles). The same linear model was used to fit the average spatial tuning data ($R^2 = 0.97 \pm 0.03$, $p < 0.05$), producing a single "V-shaped" fit in 16 of 18 cases, except for 2 cases, both in tripolar stimulation (S1 and S3), showing a "W-shaped" spatial

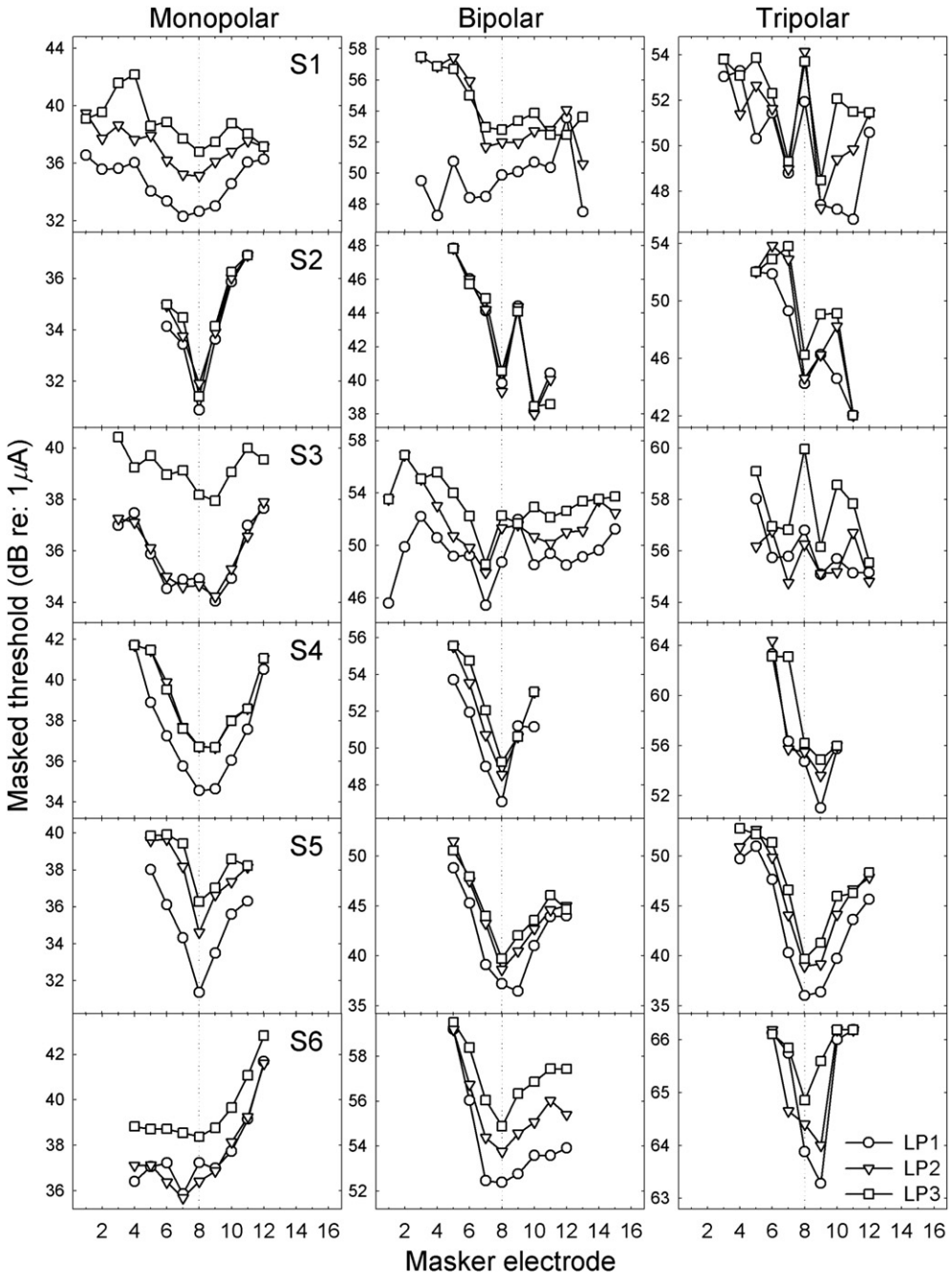


**Fig. 3.** Individual psychophysical spatial tuning curves plotting masker level as a function of masker electrode position. Rows represent individual subjects while columns represent stimulation modes. Symbols represent different probe levels. The dotted vertical line represents the probe electrode position (EL8).

tuning curve. To avoid over prediction of the narrowness of spatial tuning curve with tripolar stimulation, the combined width from the "W-shaped" tuning curve in these two subjects (S1 and S3) was used for comparison.

Stimulation mode significantly affected the spatial tuning curve bandwidth ($F_{2,51} = 3.6$, $p < 0.05$). Post-hoc analysis showed that monopolar stimulation had significantly wider spatial tuning curve width ($2.6 \pm 0.6$ EL) than bipolar stimulation ($1.1 \pm 0.4$ EL; $t_5 = 2.7$, $p < 0.05$) or tripolar stimulation ($1.8 \pm 0.5$ EL; $t_5 = 3.1$, $p < 0.05$). However, there was no significant difference in spatial tuning curve width between bipolar and tripolar stimulation ($t_5 = 1.2$, $p > 0.05$).

### 3.2. Physiological spatial masking curves

Fig. 5 shows 68 raw spatial masking curves plotting ECAP amplitude (μV) measured at a fixed-level probe (EL8) as a function of masker electrode position, with rows representing individual subjects and columns representing stimulation modes. The tripolar data in S6 could not be collected because the current amplitude exceeded the compliance limit. The four different symbols represent four different probe levels. The dotted vertical line represents the probe position at EL8. There is a great deal of individual variability in addition to variability in stimulation mode. Many spatial masking curves exhibited a peaky pattern with the peak close to the

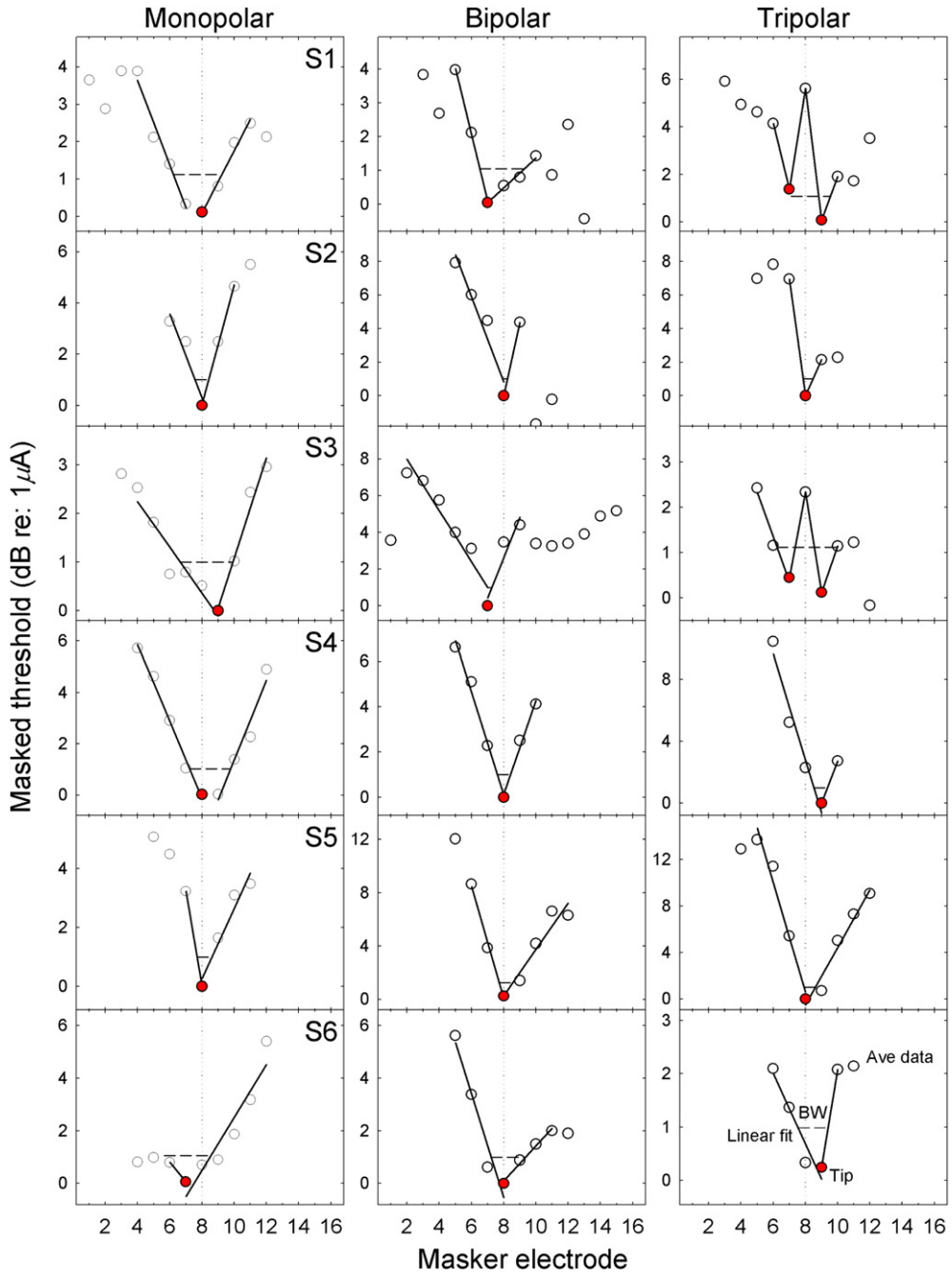


**Fig. 4.** Individual averaged spatial tuning curves (open circles) and their best fit using a linear function (solid lines). The range of the solid lines represents the electrode range used to produce the highest $R^2$ value (accounting for the most variance). The solid red symbol shows the tip position of the fitted tuning curve. The horizontal dashed line represents the $Q_{1dB}$ width of the fitted tuning curve. (For interpretation of the references to color in this figure legend, the reader is referred to the web version of this article.)

probe position (e.g., S2 monopolar, S6 bipolar, and S4 tripolar), but the spatial masking curve could either be flat (e.g., S1 monopolar) or exhibit multiple peaks (e.g., S1, S2, and S3 bipolar, S1 and S3 tripolar). Except for a few cases (e.g., S2 and S3 monopolar) where the spatial masking curve increases with probe level, most cases show no clear effect of the probe level or even decreasing spatial masking curve with probe level (e.g., S3, S4 and S6 monopolar, and S2 tripolar). The same linear model was used to fit spatial masking curves at each of the 4 probe levels ($R^2 = 0.94 \pm 0.1$, range = 0.66–1.00, $p < 0.05$). The probe level did not produce any significant effect on the mask level at the tuning tip, nor did it on the bandwidth, slope, or tip position ($F_{3,64} \leq 0.3$, $p > 0.7$). Again, the lack of probe level effect suggests that the 4 spatial masking curves be averaged to reduce variability.

Fig. 6 shows the averaged spatial masking curves over the four probe levels (circles). Overall, 12 of the 17 spatial masking curves can be fitted reasonably well by a single linear model, while the remaining 5 require two linear models (S1 all three modes, S3 bi- and tripolar modes).

Similar to the psychophysical spatial tuning curve finding, stimulation mode significantly affected the spatial masking curve width ($F_{2,65} = 5.2$, $p < 0.01$). Post-hoc analysis showed that monopolar stimulation had significantly wider spatial masking curve width (3.1 ± 0.9 EL) than bipolar stimulation (1.5 ± 0.8 EL; $t_5 = 2.7$, $p < 0.05$)

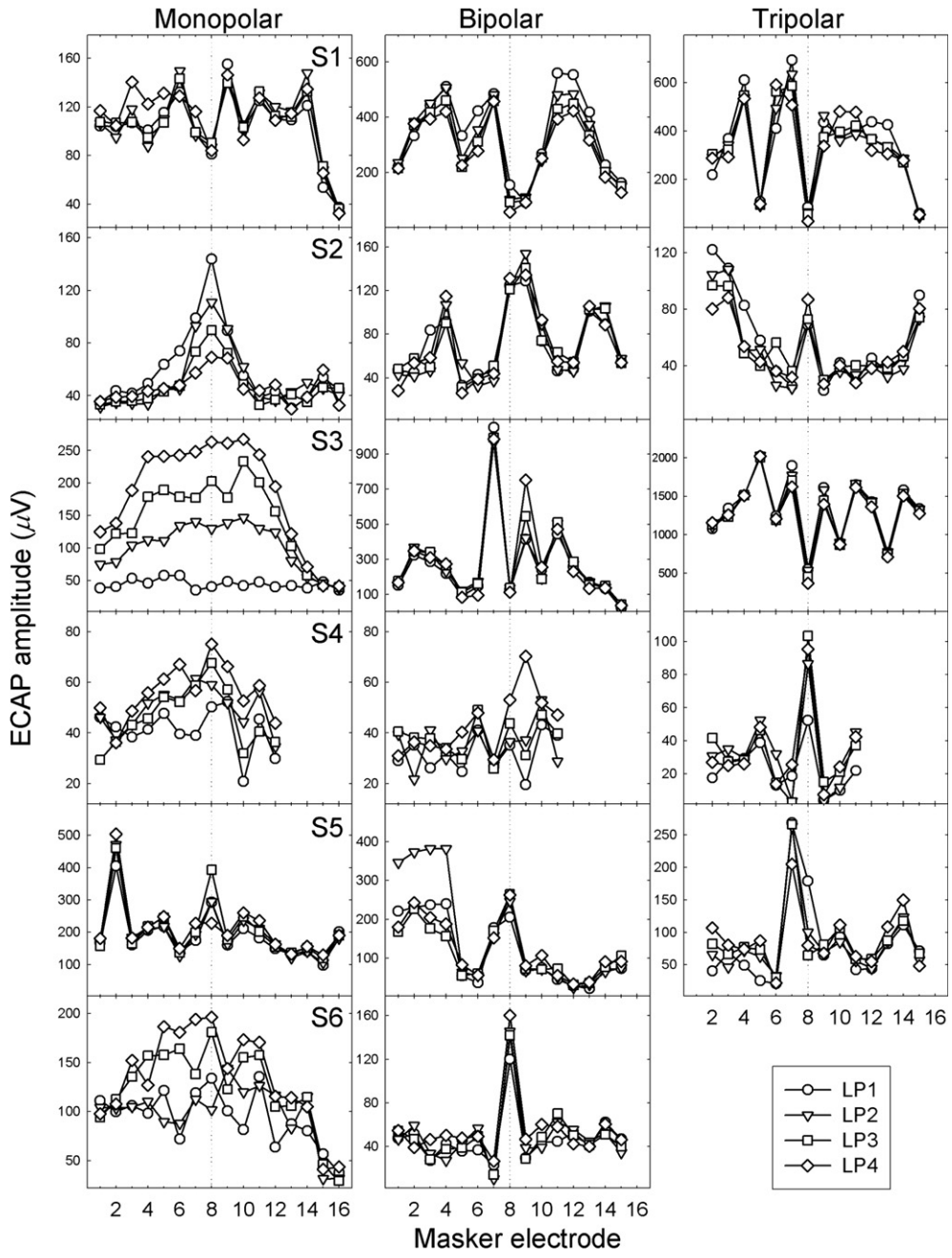


**Fig. 5.** Individual physiological spatial masking curves plotting electrically-evoked compound action potential (ECAP) amplitude as a function of masker electrode position. Rows represent individual subjects while columns represent stimulation modes. Symbols represent different probe levels. The dotted vertical line represent the probe electrode position.

and tripolar stimulation ($1.0 \pm 0.4$ EL; $t_4 = 3.9$, $p < 0.05$). However, there was no significant difference in spatial tuning curve width between bipolar and tripolar stimulation ($t_4 = 1.2$, $p > 0.05$).

### 3.3. Prediction of spatial tuning curves from spatial masking curves

Fig. 7 contrasts the predicted spatial tuning curves (solid lines) against the measured spatial tuning curves (open circles, re-plotted from Fig. 4). Spatial masking data were selected from a subset of electrodes as determined by the linear model in the spatial tuning curves (Fig. 4). These spatial masking data were then subject to a linear-logarithmic transformation (Eq. (1)) with its parameters individually adjusted to best fit the psychophysical tuning data from the same subset of electrodes (mean $R^2 = 0.75$; range = 0.46–0.97).

The top panel of Fig. 8 shows correlation between the measured spatial tuning and masking curve widths, as derived by the linear model from Figs. 4 and 6, respectively ($r = 0.75$, slope = 0.48; $p < 0.001$). Despite highly significant correlation, the shallow slope of the regression function indicates that the measured physiological masking width significantly over-estimated the actual psychophysical tuning width at small values (<2 electrodes) but under-estimated the width at larger values. The bottom panel of Fig. 8 shows that the linear-logarithmic transformation of the spatial masking curve not only improved the correlation co-efficient to 0.89, but more importantly increased the regression slope from 0.48 to 0.73, alleviating the over- and under-estimation problem with the raw physiological masking data.

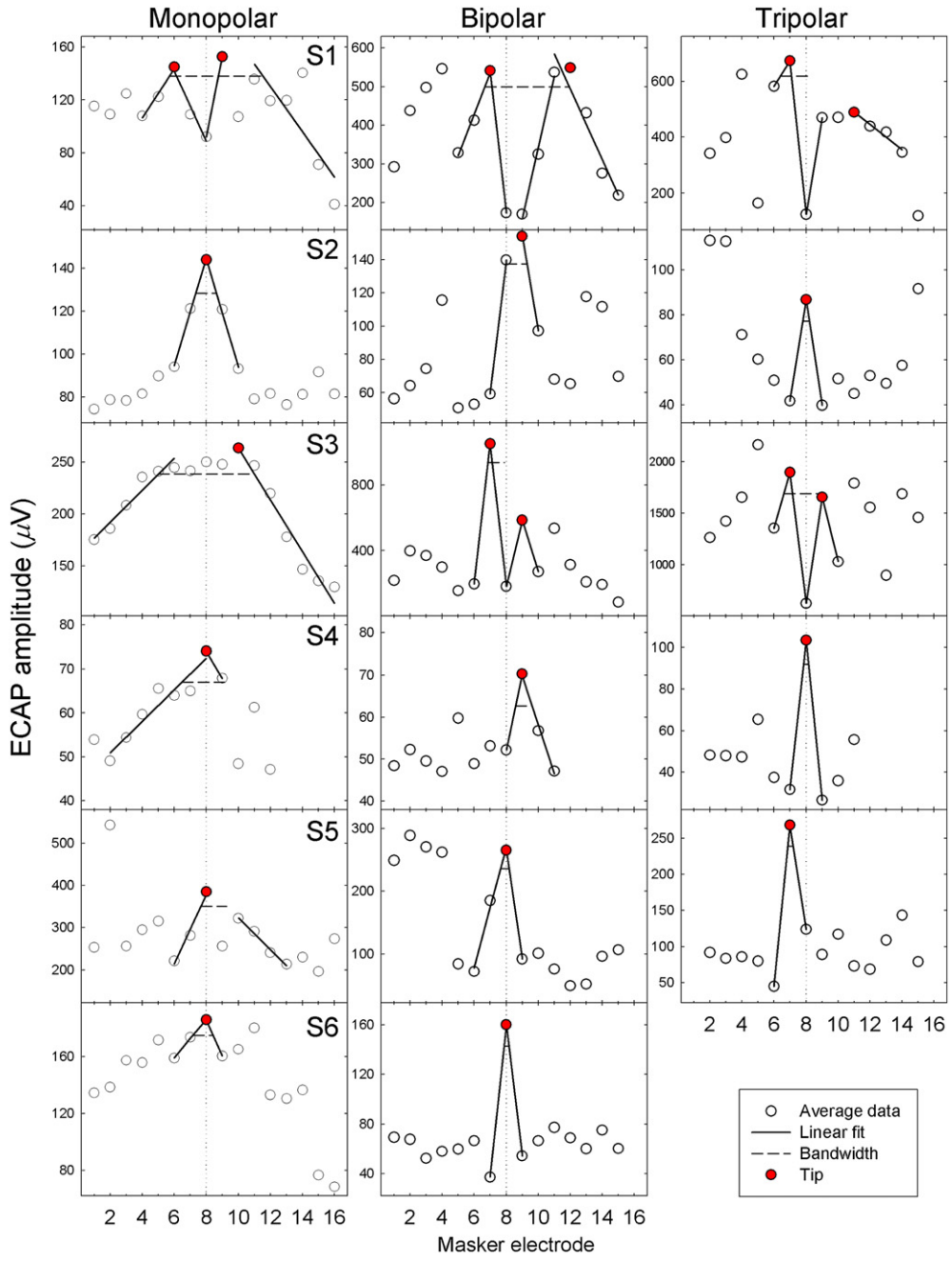


**Fig. 6.** Individual averaged spatial masking curves (open circles) and their best fit using a linear function (solid lines). The range of the solid lines represents the electrode range used to produced the highest $R^2$ value. The solid red symbol shows the peak position of the fitted tuning curve. The horizontal dashed line represents the $Q_{1dB}$ width of the fitted spatial masking curve. (For interpretation of the references to color in this figure legend, the reader is referred to the web version of this article.)

## 4. Discussion

The present study showed that, under controlled experimental conditions using the same subjects, similar procedures, similar stimuli, and controlling loudness and dynamic range, focused stimulation with either bipolar or tripolar mode produced significantly narrower spatial activity than monopolar stimulation. However, there is no significant difference between bipolar and tripolar modes. This conclusion is supported by both psychophysical and physiological data. A linear function was used to satisfactorily model the observed psychophysical spatial tuning curves and physiological spatial masking curves. Further application of a linear-logarithmic transformation of the physiological data can accurately predict the width of the individual psychophysical spatial tuning curves. Relations to previous studies and implications on underlying physiological mechanisms and clinical applications are discussed below.

### 4.1. Comparison with previous studies

Psychophysical spatial selectivity has been measured using either a fixed-level forward masker paradigm (Boex et al., 2003; Chatterjee et al., 2006; Cohen et al., 2001; Kwon and van den Honert, 2006; Shannon, 1983; Throckmorton and Collins, 1999) or

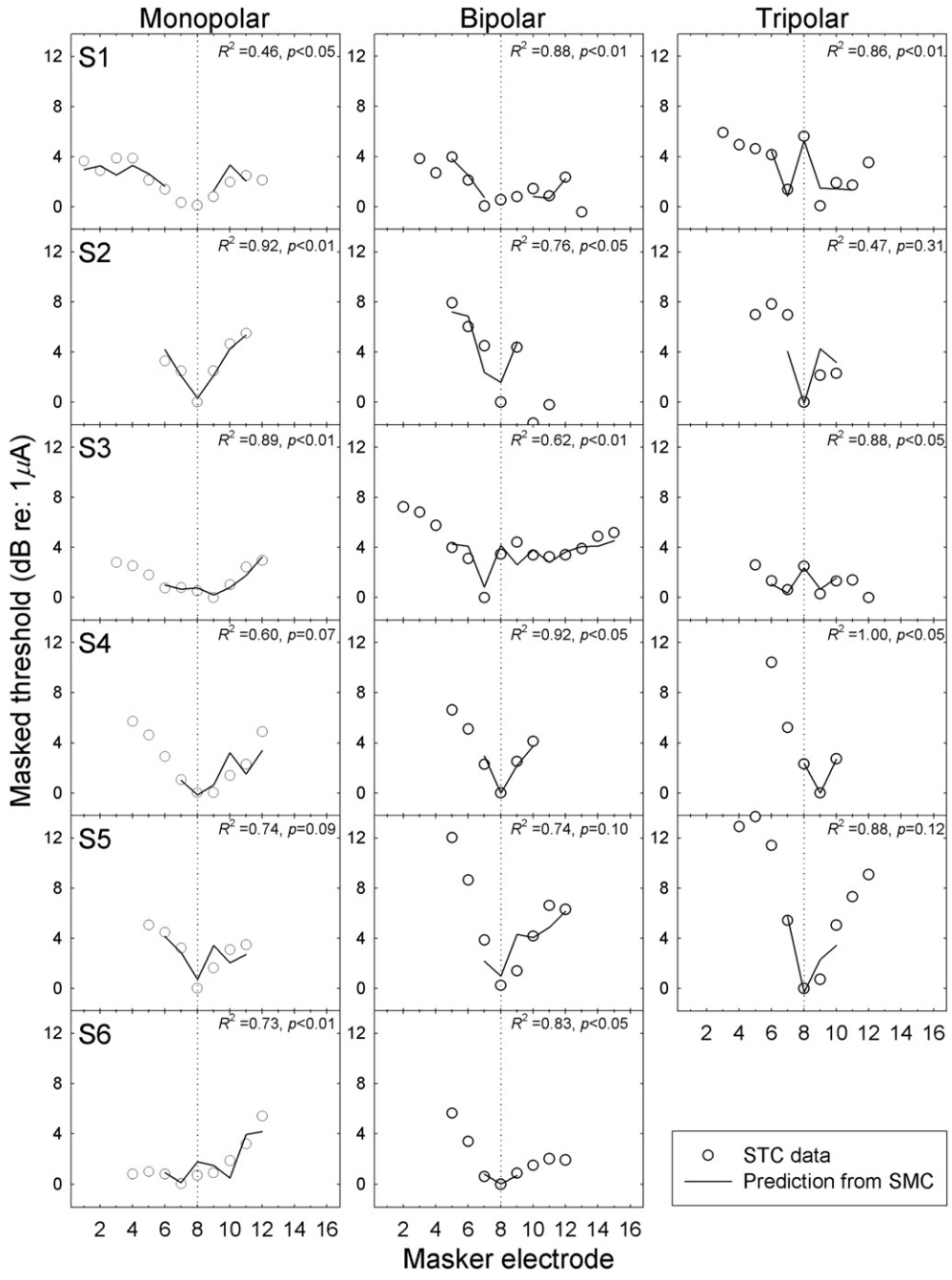


**Fig. 7.** Actual (open circles) and predicted (solid lines) psychophysical spatial tuning data by a linear-logarithmic transformation (Eq. (1) in the text) of the selected ECAP spatial masking data. The selected ECAP range was determined a subset of electrodes that best described the tip of the psychophysical tuning curve in Fig. 4.

a fixed-probe forward-masking paradigm (Bierer and Faulkner, 2010; Nelson et al., 2008). Generally speaking, the forward-masked excitation pattern measured by the first paradigm showed a relatively linear growth of masking function, a relatively small difference in the width of the excitation pattern between monopolar and bipolar stimulations, and double peaks, if the two poles in the bipolar mode were widely spaced and actually behaved like two monopoles. On the other hand, two previous studies and the current study using the second paradigm showed consistently broader spatial selectivity with monopolar mode than either bipolar or tripolar modes. They also show a shifted tip position or multiple tips of the spatial tuning curve, particularly under focused stimulation. These differences are likely reflective of a relatively high forward masker level used in the first paradigm that generates a broad excitation to "smooth" or mask any localized differences in nerve survival near the probe position. We shall return to this point in the next section discussing the underlying physiological mechanisms.

The present physiological spatial masking curve data are consistent with previous physiological studies (Abbas et al., 2004; Cohen et al., 2003; Eisen and Franck, 2005; Hughes and Stille, 2010). Similar to previous studies that measured both psychophysical and physiological spatial selectivity (Cohen et al., 2003; Hughes and Stille, 2008), the present study also found a significant correlation between the two measures. Note, however, that both previous and present studies were limited in their abilities to

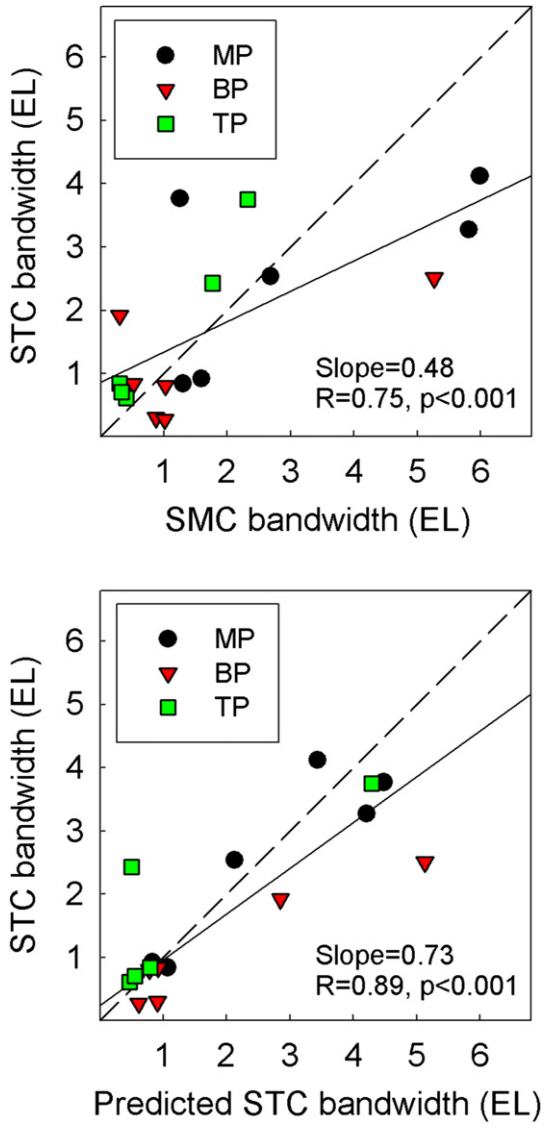


**Fig. 8.** Correlations between psychophysical and physiological spatial selectivity measures (solid circles represent monopolar data, inverted triangles represent bipolar data, and solid squares represent tripolar data). The top panel shows correlation between spatial tuning curve width (from Fig. 4) versus spatial masking curve width (from Fig. 6). The bottom panel shows correlation with predicted spatial tuning curve width by nonlinearly transforming the ECAP masking data (from Fig. 7). The dashed diagonal line represents perfect prediction of the psychophysical tuning width from the physiological data.

accurately estimate the tuning width when the tuning was sharp, particularly in bipolar and tripolar stimulation where data from 3 electrodes are used (e.g., Fig. 4: S2, S3 and S4 bipolar modes, S2, S4 and S6 tripolar modes; Fig. 6: S5 and S6 bipolar modes, S4 and S5 tripolar modes). In these cases, the tuning was effectively limited to two adjacent electrodes, a design limitation in the current cochlear implants.

### 4.2. Physiological mechanisms

First, the implication for the present data is addressed at a phenomenological level. In a normal auditory system, which is highly nonlinear, the iso-intensity and iso-response curves are not simply reversed images of one another (e.g., Ruggero, 1992). In a cochlear implant, the electric field is linear but the electrode-to-neuron interface and the central processes are not (Tang et al., 2011). The nonlinear neural-to-central transformation can be modeled by a linear-logarithmic function, with an average compression ratio ($\theta = 0.54$ in Eq. (1)) between a linear and a logarithmic function. This nonlinear transformation is likely to be related to the loudness growth difference between the pulse trains used in spatial tuning curves and the single pulses used in spatial masking curves. A modest correlation was found to account for roughly half of the variance between the slope difference of these two loudness growth functions (Fig. 2) and the degree of compression in the linear-logarithmic function used to best fit the STC data from the SMC data ($r = 0.69$, $p = 0.05$). The remaining variance might be explained by the central expansion process that converts a peripheral input into a central output (Zeng and Shannon, 1994).

Second, the overall cochlear-implant spatial selectivity must be determined by both peripheral and central factors related anatomical and physiological differences. The spatial tuning curve measure is likely to include both factors. However the spatial masking curve measure is likely to reflect peripheral irregularities, including different current spread and tissue impedance in the cochlea (Somdas et al., 2007; Vanpoucke et al., 2004), cochlear electrode placement and distance to the neurons (Finley et al., 2008; Ketten et al., 1998; Wardrop et al., 2005), and survival patterns of the degenerated neurons (Nadol et al., 2001; Spoendlin, 1984; Terayama et al., 1979). There has been well-established evidence for relating shifted or split tuning curve tip to dead region or poor nerve survival near the probe (e.g., Goldwyn et al., 2010; Moore and Alcantara, 2001).

Fig. 9 demonstrates schematically how a dead region produces shifted and split excitation patterns under focused stimulation. In cases of good and uniform nerve survival (top row), the neural responses (curves) simply reflects the broad electric field with monopolar stimulation (the shaded area in the left panel) or the narrow electric field with focused stimulation such as bipolar and tripolar mode (the relatively narrower shaded area in the right panel). In cases of poor nerve survival (bottom two rows), the broad stimulation can still excite a large number of residual neurons, showing perhaps an overall reduction, but with no shift or split in excitation pattern. However, the focused stimulation would produce a shifted excitation pattern if it mostly excites residual neurons on one side (left-middle panel) or an excitation pattern with split peaks if it excites residual neurons on both sides of the dead region.

### 4.3. Clinical applications

This section discusses how this improved understanding of cochlear-implant spatial selectivity can help account for clinical results and develop new clinical tools. First, it is clear that focused stimulation is not necessarily a good thing for all cochlear-implant users or all electrode locations in an individual user. If a user has one or multiple dead regions due to irregular nerve survival patterns, focused stimulation will likely produce mismatched or overlapping frequency-to-place maps as a result of shifted or split excitation patterns. Such mismatches and overlaps will likely degrade speech performance (e.g., Shannon et al., 1998), which probably explains the lack of performance benefits observed in studies using focused stimulation (Donaldson et al., 2011; Hughes and Stille, 2008; Mens and Berenstein, 2005; Pfingst et al., 2001). In other words, the mismatching and overlapping frequency-to-place maps will likely wipe out any potential benefit of increased spatial selectivity with focused stimulation because essentially all implant users will have some degrees of nerve degeneration. This tradeoff can also explain the apparent discrepancy between the

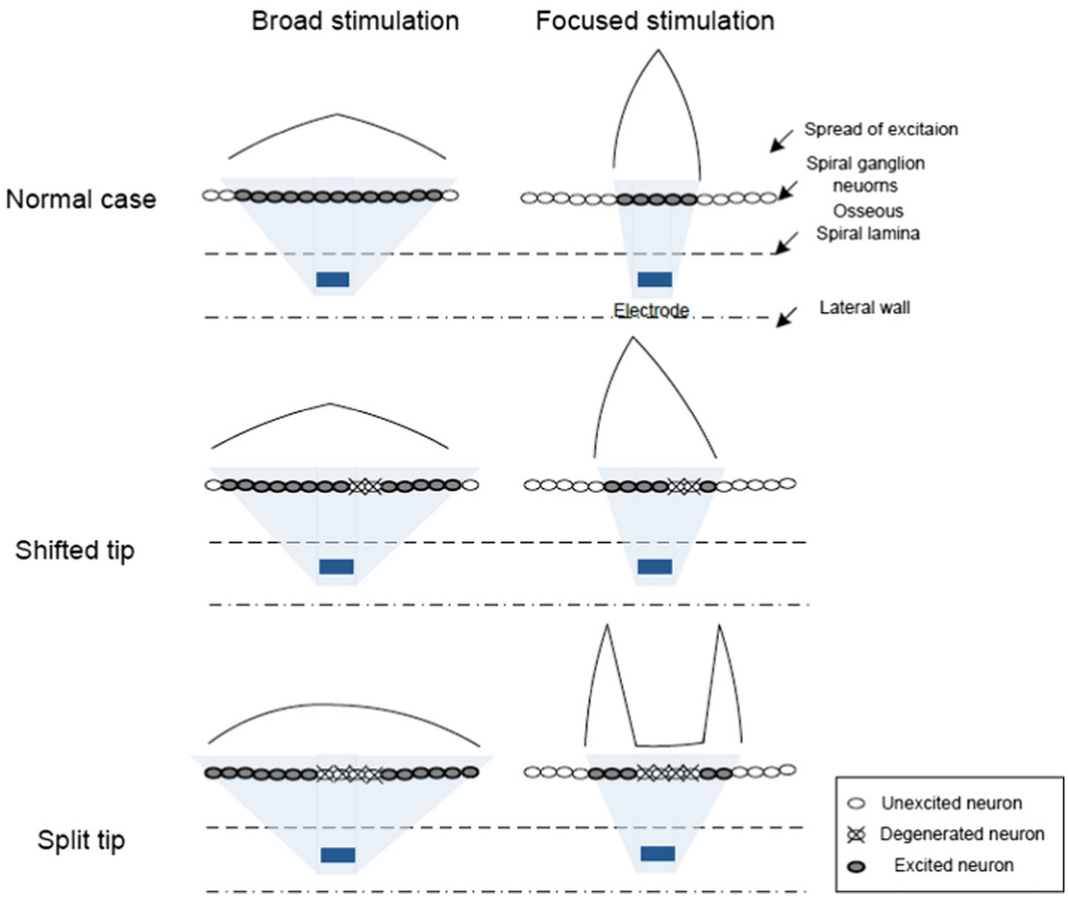


**Fig. 9.** Schematic excitation patterns of broad (left column) and focused (right column) electric stimulation (shaded area) and its interactions with nerve survival patterns (row 1 = good survival; rows 2 and 3 = poor survival). See text for details.

human implant data and the animal implant data showing uniformly increased spatial selectivity with focused stimulation because the animals studied were acutely deafened and likely to have good nerve survival (e.g., Bierer and Middlebrooks, 2002).

On the other hand, identification of shifted or split excitation patterns could potentially solve this tradeoff problem with focused stimulation. Imagine a custom fitting system where spatial selectivity is measured using focused stimulation in all electrode position and different stimulation modes are employed dependent upon the status of nerve survival. In cochlear regions with good nerve survival, focused stimulation can be employed to take advantage of increased spatial selectivity; whereas in regions with poor nerve survival, focused stimulation can be either adjusted to a new place or avoided altogether using broad stimulation. Cochlear-implant performance may be improved under this type of custom fitting, but, unfortunately, no commercially available devices currently support this multi-mode stimulation.

The successful prediction of the psychophysical spatial tuning curve by the physiological spatial masking curve is of high clinical significance. First, the psychophysical test is much longer and potentially less reliable than the physiological test. It would take longer than 200 min (4 min per run $\times$ 3 runs $\times$ 16 electrode + rest time to avoid fatigue) to obtain a single spatial tuning curve, while shorter than 20 min to obtain a comparable spatial masking curve (1 min for 64 automatic sweeps per electrode $\times$ 16 electrodes + no rest time needed). Second, as the minimum age for implantation continues to decrease while the inclusion criteria continue to expand, the psychophysical test may be challenging or even impossible for the pediatric and expanded populations. The objective physiological measure is relatively reliable, fast and requires no subjective responses, which makes it useful to not only predict threshold and maximal loudness, but also spatial selectivity in cochlear implants (e.g., Eisen and Franck, 2004; Gartner et al., 2010). Combining these physiological measures could allow efficient and effective fitting of the cochlear implant and improve its overall performance.

## Acknowledgment

The authors thank all subjects for their time and dedication. The authors also thank Matthew Chang, Grace Hunter and two anonymous reviewers for comments on the manuscript. The experiments were supported by the NIH grants (RO1-DC008858 and P30-DC008369), the Scholarship of the Ministry of Education of China, and the Natural Science Fund of China (30800234 and 60871083).

## References

Abbas, P.J., Hughes, M.L., Brown, C.J., Miller, C.A., South, H., 2004. Channel interaction in cochlear implant users evaluated using the electrically evoked compound action potential. Audiol Neurootol 9, 203–213.

Abbas, P.J., Brown, C.J., Shallop, J.K., Firszt, J.B., Hughes, M.L., Hong, S.H., Staller, S.J., 1999. Summary of results using the nucleus CI24M implant to record the electrically evoked compound action potential. Ear Hear 20, 45–59.

Bekesy, G., 1952. Direct observation of the vibrations of the cochlear partition under a microscope. Acta Otolaryngol 42, 197–201.

Berenstein, C.K., Mens, L.H., Mulder, J.J., Vanpoucke, F.J., 2008. Current steering and current focusing in cochlear implants: comparison of monopolar, tripolar, and virtual channel electrode configurations. Ear Hear 29, 250–260.

Berenstein, C.K., Vanpoucke, F.J., Mulder, J.J., Mens, L.H., 2010. Electrical field imaging as a means to predict the loudness of monopolar and tripolar stimuli in cochlear implant patients. Hear Res 270, 28–38.
Bierer, J.A., Middlebrooks, J.C., 2002. Auditory cortical images of cochlear-implant stimuli: dependence on electrode configuration. J Neurophysiol 87, 478–492.
Bierer, J.A., Faulkner, K.F., 2010. Identifying cochlear implant channels with poor electrode-neuron interface: partial tripolar, single-channel thresholds and psychophysical tuning curves. Ear Hear 31, 247–258.
Bierer, J.A., Bierer, S.M., Middlebrooks, J.C., 2010. Partial tripolar cochlear implant stimulation: spread of excitation and forward masking in the inferior colliculus. Hear Res 270, 134–142.
Boex, C., Kos, M.I., Pelizzone, M., 2003. Forward masking in different cochlear implant systems. J Acoust Soc Am 114, 2058–2065.
Bonham, B.H., Litvak, L.M., 2008. Current focusing and steering: modeling, physiology, and psychophysics. Hear Res 242, 141–153.
Brown, C.J., Hughes, M.L., Luk, B., Abbas, P.J., Wolaver, A., Gervais, J., 2000. The relationship between EAP and EABR thresholds and levels used to program the nucleus 24 speech processor: data from adults. Ear Hear 21, 151–163.
Chatterjee, M., Shannon, R.V., 1998. Forward masked excitation patterns in multielectrode electrical stimulation. J Acoust Soc Am 103, 2565–2572.
Chatterjee, M., Galvin, J.J., Fu, Q.J., Shannon, R.V., 2006. Effects of stimulation mode, level and location on forward-masked excitation patterns in cochlear implant patients. J Assoc Res Otolaryngol 7, 15–25.
Chistovich, L.A., 1957. Frequency characteristics of the masking effect. Biofizika 2, 714–725.
Chua, T.E., Bachman, M., Zeng, F.G., 2011. Intensity coding in electric hearing: effects of electrode configurations and stimulation waveforms. Ear Hear 32 (6), 679–689.
Cohen, L.T., Saunders, E., Clark, G.M., 2001. Psychophysics of a prototype perimodiolar cochlear implant electrode array. Hear Res 155, 63–81.
Cohen, L.T., Richardson, L.M., Saunders, E., Cowan, R.S., 2003. Spatial spread of neural excitation in cochlear implant recipients: comparison of improved ECAP method and psychophysical forward masking. Hear Res 179, 72–87.
Cullington, H.E., Zeng, F.G., 2010. Bimodal hearing benefit for speech recognition with competing voice in cochlear implant subject with normal hearing in contralateral ear. Ear Hear 31, 70–73.
de Sauvage, R.C., Cazals, Y., Erre, J.P., Aran, J.M., 1983. Acoustically derived auditory nerve action potential evoked by electrical stimulation: an estimation of the waveform of single unit contribution. J Acoust Soc Am 73, 616–627.
Dillier, N., Lai, W.K., Almqvist, B., Frohne, C., Muller-Deile, J., Stecker, M., von Wallenberg, E., 2002. Measurement of the electrically evoked compound action potential via a neural response telemetry system. Ann Otol Rhinol Laryngol 111, 407–414.
Dingemanse, J.G., Frijns, J.H., Briaire, J.J., 2006. Psychophysical assessment of spatial spread of excitation in electrical hearing with single and dual electrode contact maskers. Ear Hear 27, 645–657.
Donaldson, G.S., Viemeister, N.F., Nelson, D.A., 1997. Psychometric functions and temporal integration in electric hearing. J Acoust Soc Am 101, 3706–3721.
Donaldson, G.S., Dawson, P.K., Borden, L.Z., 2011. Within-subjects comparison of the HiRes and Fidelity120 speech processing strategies: speech perception and its relation to place-pitch sensitivity. Ear Hear 32, 238–250.
Eisen, M.D., Franck, K.H., 2004. Electrically evoked compound action potential amplitude growth functions and HiResolution programming levels in pediatric CII implant subjects. Ear Hear 25, 528–538.
Eisen, M.D., Franck, K.H., 2005. Electrode interaction in pediatric cochlear implant subjects. J Assoc Res Otolaryngol 6, 160–170.
Finley, C.C., Holden, T.A., Holden, L.K., Whiting, B.R., Chole, R.A., Neely, G.J., Hullar, T.E., Skinner, M.W., 2008. Role of electrode placement as a contributor to variability in cochlear implant outcomes. Otol Neurotol 29, 920–928.
Fishman, K.E., Shannon, R.V., Slattery, W.H., 1997. Speech recognition as a function of the number of electrodes used in the SPEAK cochlear implant speech processor. J Speech Lang Hear Res 40, 1201–1215.
Fletcher, H., 1935. Newer concepts of the pitch, the loudness, and the timbre of musical tones. J Franklin Inst 220, 405–429.
Friesen, L.M., Shannon, R.V., Baskent, D., Wang, X., 2001. Speech recognition in noise as a function of the number of spectral channels: comparison of acoustic hearing and cochlear implants. J Acoust Soc Am 110, 1150–1163.
Fu, Q.J., 2005. Loudness growth in cochlear implants: effect of stimulation rate and electrode configuration. Hear Res 202, 55–62.
Gartner, L., Lenarz, T., Joseph, G., Buchner, A., 2010. Clinical use of a system for the automated recording and analysis of electrically evoked compound action potentials (ECAPs) in cochlear implant patients. Acta Otolaryngol 130, 724–732.
Goldwyn, J.H., Bierer, S.M., Bierer, J.A., 2010. Modeling the electrode–neuron interface of cochlear implants: effects of neural survival, electrode placement, and the partial tripolar configuration. Hear Res 268, 93–104.
Helmholtz, H.L.F., 1877. On the Sensations of Tone, second English ed. Dover, New York.
Henry, B.A., Turner, C.W., 2003. The resolution of complex spectral patterns by cochlear implant and normal-hearing listeners. J Acoust Soc Am 113, 2861–2873.
Hughes, M.L., Stille, L.J., 2008. Psychophysical versus physiological spatial forward masking and the relation to speech perception in cochlear implants. Ear Hear 29, 435–452.
Hughes, M.L., Stille, L.J., 2010. Effect of stimulus and recording parameters on spatial spread of excitation and masking patterns obtained with the electrically evoked compound action potential in cochlear implants. Ear Hear 31, 679–692.
Jolly, C.N., Spelman, F.A., Clopton, B.M., 1996. Quadrupolar stimulation for cochlear prostheses: modeling and experimental data. IEEE Trans Biomed Eng 43, 857–865.
Ketten, D.R., Skinner, M.W., Wang, G., Vannier, M.W., Gates, G.A., Neely, J.G., 1998. In vivo measures of cochlear length and insertion depth of nucleus cochlear implant electrode arrays. Ann Otol Rhinol 107, 1–16.
Khan, A.M., Whiten, D.M., Nadol Jr., J.B., Eddington, D.K., 2005. Histopathology of human cochlear implants: correlation of psychophysical and anatomical measures. Hear Res 205, 83–93.
Koch, D.B., Osberger, M.J., Segel, P., Kessler, D., 2004. HiResolution and conventional sound processing in the HiResolution bionic ear: using appropriate outcome measures to assess speech recognition ability. Audiol Neurootol 9, 214–223.
Kral, A., Hartmann, R., Mortazavi, D., Klinke, R., 1998. Spatial resolution of cochlear implants: the electrical field and excitation of auditory afferents. Hear Res 121, 11–28.
Kwon, B.J., van den Honert, C., 2006. Effect of electrode configuration on psychophysical forward masking in cochlear implant listeners. J Acoust Soc Am 119, 2994–3002.
Levitt, H., 1971. Transformed up-down methods in psychoacoustics. J Acoust Soc Am 49 (Suppl. 2), 467.
Liberman, M.C., Dodds, L.W., 1984. Single-neuron labeling and chronic cochlear pathology. III. Stereocilia damage and alterations of threshold tuning curves. Hear Res 16, 55–74.
Lim, H.H., Tong, Y.C., Clark, G.M., 1989. Forward masking patterns produced by intracochlear electrical stimulation of one and two electrode pairs in the human cochlea. J Acoust Soc Am 86, 971–980.
Linthicum Jr., F.H., Fayad, J., Otto, S.R., Galey, F.R., House, W.F., 1991. Cochlear implant histopathology. Am J Otol 12, 245–311.
Litvak, L.M., Spahr, A.J., Emadi, G., 2007a. Loudness growth observed under partially tripolar stimulation: model and data from cochlear implant listeners. J Acoust Soc Am 122, 967–981.
Litvak, L.M., Spahr, A.J., Saoji, A.A., Fridman, G.Y., 2007b. Relationship between perception of spectral ripple and speech recognition in cochlear implant and vocoder listeners. J Acoust Soc Am 122, 982–991.
Mens, L.H., Berenstein, C.K., 2005. Speech perception with mono- and quadrupolar electrode configurations: a crossover study. Otol Neurotol 26, 957–964.
Middlebrooks, J.C., Bierer, J.A., 2002. Auditory cortical images of cochlear-implant stimuli: coding of stimulus channel and current level. J Neurophysiol 87, 493–507.
Miller, C.A., Abbas, P.J., Brown, C.J., 2000. An improved method of reducing stimulus artifact in the electrically evoked whole-nerve potential. Ear Hear 21, 280–290.
Miller, C.A., Abbas, P.J., Nourski, K.V., Hu, N., Robinson, B.K., 2003. Electrode configuration influences action potential initiation site and ensemble stochastic response properties. Hear Res 175, 200–214.
Moore, B.C., Glasberg, B.R., 1986. Comparisons of frequency selectivity in simultaneous and forward masking for subjects with unilateral cochlear impairments. J Acoust Soc Am 80, 93–107.
Moore, B.C., Alcantara, J.I., 2001. The use of psychophysical tuning curves to explore dead regions in the cochlea. Ear Hear 22, 268–278.
Nadol Jr., J.B., Shiao, J.Y., Burgess, B.J., Ketten, D.R., Eddington, D.K., Gantz, B.J., Kos, I., Montandon, P., Coker, N.J., Roland Jr., J.T., Shallop, J.K., 2001. Histopathology of cochlear implants in humans. Ann Otol Rhinol Laryngol 110, 883–891.
Nelson, D.A., Donaldson, G.S., 2002. Psychophysical recovery from pulse-train forward masking in electric hearing. J Acoust Soc Am 112, 2932–2947.
Nelson, D.A., Donaldson, G.S., Kreft, H., 2008. Forward-masked spatial tuning curves in cochlear implant users. J Acoust Soc Am 123, 1522–1543.
Pfingst, B.E., Xu, L., 2004. Across-site variation in detection thresholds and maximum comfortable loudness levels for cochlear implants. J Assoc Res Otolaryngol 5, 11–24.
Pfingst, B.E., Franck, K.H., Xu, L., Bauer, E.M., Zwolan, T.A., 2001. Effects of electrode configuration and place of stimulation on speech perception with cochlear prostheses. J Assoc Res Otolaryngol 2, 87–103.
Pickles, J.O., 1988. An Introduction to the Physiology of Hearing, second ed. Academic Press, London.
Plomp, R., 1964. The ear as a frequency analyzer. J Acoust Soc Am 36, 1628–1636.
Raggio, M.W., Schreiner, C.E., 1994. Neuronal responses in cat primary auditory cortex to electrical cochlear stimulation. I. Intensity dependence of firing rate and response latency. J Neurophysiol 72, 2334–2359.
Ruggero, M.A., 1992. Responses to sound of the basilar membrane of the mammalian cochlea. Curr Opin Neurobiol 2, 449–456.
Saoji, A.A., Litvak, L.M., Hughes, M.L., 2009. Excitation patterns of simultaneous and sequential dual-electrode stimulation in cochlear implant recipients. Ear Hear 30, 559–567.
Shannon, R.V., 1983. Multichannel electrical stimulation of the auditory nerve in man. II. Channel interaction. Hear Res 12, 1–16.
Shannon, R.V., 1985. Threshold and loudness functions for pulsatile stimulation of cochlear implants. Hear Res 18, 135–143.
Shannon, R.V., Zeng, F.G., Wygonski, J., 1998. Speech recognition with altered spectral distribution of envelope cues. J Acoust Soc Am 104, 2467–2476.
Small, A.M., 1959. Pure-tone masking. J Acoust Soc Am 31, 1619–1625.
Snyder, R.L., Middlebrooks, J.C., Bonham, B.H., 2008. Cochlear implant electrode configuration effects on activation threshold and tonotopic selectivity. Hear Res 235, 23–38.
Somdas, M.A., Li, P.M., Whiten, D.M., Eddington, D.K., Nadol Jr., J.B., 2007. Quantitative evaluation of new bone and fibrous tissue in the cochlea following cochlear implantation in the human. Audiol Neurootol 12, 277–284.

Spoendlin, H., 1984. Factors inducing retrograde degeneration of the cochlear nerve. Ann Otol Rhinol Laryngol Suppl 112.
Srinivasan, A.G., Landsberger, D.M., Shannon, R.V., 2010. Current focusing sharpens local peaks of excitation in cochlear implant stimulation. Hear Res 270, 89–100.
Tang, Q., Benitez, R., Zeng, F.G., 2011. Spatial channel interactions in cochlear implants. J Neural Eng 8, 046029.
Tasaki, I., 1954. Nerve impulses in individual auditory nerve fibers of guinea pig. J Neurophysiol 17, 97–122.
Terayama, Y., Kaneko, K., Tanaka, K., Kawamoto, K., 1979. Ultrastructural changes of the nerve elements following disruption of the organ of Corti. II. Nerve elements outside the organ of Corti. Acta Otolaryngol Suppl 88, 27–36.
Throckmorton, C.S., Collins, L.M., 1999. Investigation of the effects of temporal and spatial interactions on speech-recognition skills in cochlear-implant subjects. J Acoust Soc Am 105, 861–873.
Tykocinski, M., Saunders, E., Cohen, L.T., Treaba, C., Briggs, R.J., Gibson, P., Clark, G.M., Cowan, R.S., 2001. The contour electrode array: safety study and initial patient trials of a new perimodiolar design. Otol Neurotol 22, 33–41.
van den Honert, C., Stypulkowski, P.H., 1987. Single fiber mapping of spatial excitation patterns in the electrically stimulated auditory nerve. Hear Res 29, 195–206.
Vanpoucke, F., Zarowski, A., Casselman, J., Frijns, J., Peeters, S., 2004. The facial nerve canal: an important cochlear conduction path revealed by Clarion electrical field imaging. Otol Neurotol 25, 282–289.
Vollmer, M., Beitel, R.E., Snyder, R.L., Leake, P.A., 2007. Spatial selectivity to intracochlear electrical stimulation in the inferior colliculus is degraded after long-term deafness in cats. J Neurophysiol 98, 2588–2603.
Wardrop, P., Whinney, D., Rebscher, S.J., Luxford, W., Leake, P., 2005. A temporal bone study of insertion trauma and intracochlear position of cochlear implant electrodes. II: comparison of Spiral Clarion and HiFocus II electrodes. Hear Res 203, 68–79.
Wilson, B.S., Finley, C.C., Lawson, D.T., Wolford, R.D., Eddington, D.K., Rabinowitz, W.M., 1991. Better speech recognition with cochlear implants. Nature 352, 236–238.
Won, J.H., Drennan, W.R., Rubinstein, J.T., 2007. Spectral-ripple resolution correlates with speech reception in noise in cochlear implant users. J Assoc Res Otolaryngol 8, 384–392.
Zeng, F.G., 2004. Trends in cochlear implants. Trends Amplif 8, 1–34.
Zeng, F.G., Shannon, R.V., 1992. Loudness balance between electric and acoustic stimulation. Hear Res 60, 231–235.
Zeng, F.G., Shannon, R.V., 1994. Loudness-coding mechanisms inferred from electric stimulation of the human auditory system. Science 264, 564–566.
Zeng, F.G., Galvin 3rd, J.J., Zhang, C., 1998. Encoding loudness by electric stimulation of the auditory nerve. Neuroreport 9, 1845–1848.
Zeng, F.G., Tang, Q., Dimitrijevic, A., Starr, A., Larky, J., Blevins, N.H., 2011. Tinnitus suppression by low-rate electric stimulation and its electrophysiological mechanisms. Hear Res 277, 61–66.
Zhu, Z., Tang, Q., Zeng, F.G., Guan, T., Ye, D.T., 2010. Electric field imaging of monopolar, bipolar and tripolar modes of electric stimuli in cochlear implant users. J Tsinghua Univ (Sci Technol) 50, 1440–1444.
Zwicker, E., 1974. On a psychoacoustic equivalent of tuning curves. In: Zwickcr, E., Terhardt, E. (Eds.), Facts and Models in Hearing. Springer-Verlag, Heidelberg.